School of Pharmaceutical Sciences[1], Center of Laboratory Animals[2], Sun Yat-sen University, Guangzhou; Qingyuan People's Hospital[3], Qingyuan, PR China

Necroptosis contributes to the cyclosporin A-induced cytotoxicity in NRK-52E cells

Zizhang Ouyang[1,2], Shaohua Zhu[1], Jing Jin[1], Jia Li[1], Yuwen Qiu[1], Min Huang[1], Zhiying Huang[1,2]

Received December 8, 2011, accepted January 6, 2012

Zhiying Huang, School of Pharmaceutical sciences, Sun Yat-sen University, Guangzhou 510006, PR China hzhiying@mail.sysu.edu.cn

Pharmazie 67: 725–732 (2012) *doi: 10.1691/ph.2012.1837*

Cyclosporin A (CsA) induces renal tubular epithelial cells apoptosis and necrosis following *in vitro* exposure. The mechanisms of CsA-induced apoptosis have been studied intensively, whereas the mechanisms of necrosis remain to be elucidated. Necroptosis has been described as programmed necrosis. This study investigated the ability of CsA to induce necroptosis in the rat tubular cell line NRK-52E. The NRK-52E cells were incubated with CsA for 24 hours with or without necrostatin-1 (Nec-1). The majority of the NRK-52E cells died of necrosis as indicated by LDH leakage, Hoechst 33342/PI staining, and flow cytometry analysis. Cell death was significantly reduced by Nec-1 pretreated before CsA exposure. CsA-induced apoptosis and necrosis were also compared in NRK-52E cells with or without knockdown of receptor interaction protein 3 (RIP3) expression using small interfering RNA. Moreover, the role of reactive oxygen species (ROS) in CsA-induced cell death was also attempted. The result suggests that necroptosis contributes to the CsA-induced cytotoxicity in NRK-52E cells. Meanwhile, RIP3 and ROS are involved in CsA-induced necroptosis. To our knowledge, this is the first report on necroptosis in CsA-induced renal tubular cell death pathways, which might offer a novel protective target for CsA nephrotoxicity.

1. Introduction

The immunosuppressive agent cyclosporin A (CsA) is widely used to prevent rejection in various types of organ transplantation and in the treatment of various autoimmune disorders (Kahan 1992; Borel et al. 1996). However, CsA therapy is associated with severe renal injury, which significantly limits its clinical utilization (Myers et al. 1988; Nakamura et al. 2007). The pathogenesis of CsA nephrotoxicity has been thought to be secondary to the hemodynamic changes elicited by its intense effect on vasoconstriction (Racusen 1993). However, increasing evidence also indicates that CsA has a direct toxicity to renal tubular cells (Mihatsch et al. 1986; Nickeleit et al. 1998). Low dose CsA (4.2 nM) has been shown to induce apoptosis, whereas high doses CsA (21 μM or greater) induced necrosis in a porcine kidney cell line (LLC-PK1 cells) (Healy et al. 1998). Another investigation indicated that the cellular viability of cultured adult human proximal tubular epithelial cells (PTEC) is not influenced by short-term CsA exposure at physiological concentrations. At very high drug concentrations, cultured human PTEC cells die of cell necrosis, an effect that might solely be based on vehicle toxicity (Bakker et al. 2002). Therefore, the mechanism for CsA-induced cytotoxicity is still controversial, and the molecular mechanism remains undefined.

Cell death is usually classified as apoptosis or necrosis. Apoptosis is a controlled cellular process, also known as "programmed cell death" or "cell suicide." In contrast, necrosis is thought to be uncontrolled passive cell death caused by overwhelming stress (Majno and Joris 1995). Recently, Degterev et al. demonstrated a new cell death pathway termed as "necroptosis" and this cell death process has been shown to be inhibited specifically by Nec-1. Nec-1 is now considered as a powerful tool for distinguishing necroptosis from other forms of cell death, although the exact mechanisms of necroptosis are still unclear (Degterev et al. 2005; Teng et al. 2005). RIP3 plays an important role during cell death and it is primitively identified as a protein kinase that induces cellular apoptosis through its overexpression (Yu et al. 1999). Zhang et al. (2009) have demonstrated that upregulation of cellular energy metabolism by RIP3 increases ROS production in the mitochondrial respiratory chain, consequently leading to necroptosis. To our knowledge, whether RIP3 participates in renal proximal tubular cell death induced by CsA has not been studied.

Therefore, the current study investigated the involvement of necroptosis in CsA cytotoxicity on rat renal proximal tubular epithelial cells. Moreover, we attempted to find out the role of RIP3 in CsA-induced cell necroptosis.

2. Investigations and results

2.1. CsA causes apoptotic and necrotic renal cell death

As shown in Fig. 1 and 2A, 24 h incubation of the rat renal proximal tubular cell line NRK-52E with CsA produced a concentration-dependent loss of cell viability and increased cell death as demonstrated by the decreased reduction of MTT and increased LDH release, respectively. MTT reduction was observed using CsA concentrations of 5 μM or greater. In accordance with the MTT results, significant LDH release was detected at 5 μM CsA. The results suggest that necrotic cell death occurred at CsA concentrations of 5 μM or greater. The

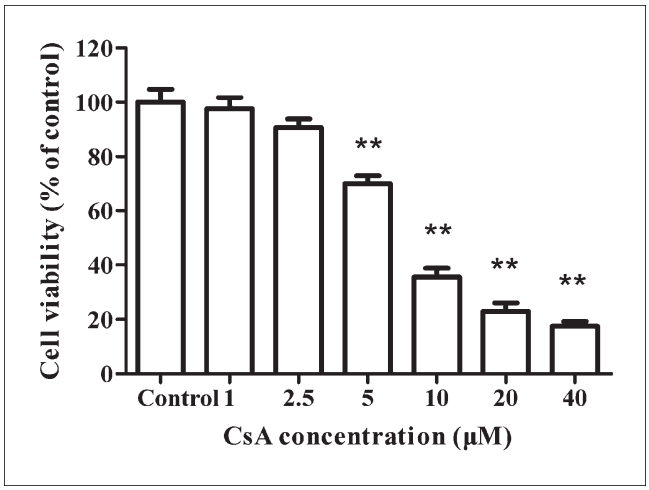

Fig. 1: Effect of CsA on cell viability. NRK-52E cells were incubated without or with CsA (1, 2.5, 10, 20, and 40 μM) for 24 h. The cell viability was determined via an MTT assay. All data are presented as means ± SD from at least three independent experiments performed in triplicate (**$P < 0.01$ vs. the control group)

confirmation of necrosis was made using a combination of Hoechst 33342/PI double staining to determine nuclear morphology and membrane integrity. At 5 μM, CsA produced a significant increase in apoptotic cell death (Fig. 3A); at 10 μM, CsA produced a significant increase in both apoptotic and necrotic cell death; more cells were necrotic than apoptotic (Fig. 3A).

2.2. Nec-1 protected against CsA-induced cytotoxicity in NRK-52E cells

The release of LDH from the cell cytoplasm is a marker for necrotic cell death. As depicted in Fig. 2B, 24 h exposure to 10 μM CsA resulted in marked LDH release from the cells. In contrast, pretreatment of the cells with Nec-1, a specific inhibitor of necroptosis, effectively inhibited CsA-induced LDH release in a concentration-dependent manner. Furthermore, 100 μM Nec-1 almost reversed the augment effects of CsA on extracellular LDH activity. In contrast, z-VAD-fmk, a pancaspase inhibitor, partly suppressed LDH levels in the culture medium. These results indicate that necroptosis is involved in CsA-induced cytotoxicity. Furthermore, Nec-1 also clearly protected CsA-induced changes in cell and nuclear morphology. A decrement was found for the number of necrotic cells but not for that of apoptotic or late apoptotic cell (Fig. 3B). These results also indicate that necroptosis is involved in the induction mechanism of CsA-induced cell death. To confirm further the protective role of Nec-1, CsA-induced apoptosis and necrosis in NRK-52E cells were assessed through flow cytometry. As shown in Fig. 4, both the percentage of early apoptotic and late apoptotic/necrotic NRK-52E cells significantly increased after treatment with CsA (10 μM) for 24 h compared with the control. Nec-1, as a specific necroptotic inhibitor, significantly decreased the number of CsA-induced late apoptotic/necrotic cells. In contrast, Nec-1 did not reduce CsA-induced early apoptotic cell death. The results were consistent with the reports of other researchers that Nec-1 is a specific inhibitor of programmed necrosis, but not of apoptosis (Degterev et al. 2005; Han et al. 2009). As expected, pancaspase inhibitor z-VAD-fmk decreased the percentage of CsA-induced apoptotic cells (Fig. 3B and 4). It did not completely inhibit CsA-induced cell death, which indicates that another form of cell death occurred aside from apoptosis.

2.3. RIP3 was involved in CsA-induced necroptosis in NRK-52E cells

As shown in Fig. 5, the RIP3 protein level was downregulated significantly by RIP3-siRNA treatment. Flow cytometry analysis showed that when RIP3-siRNA transfected NRK-52E cells were treated with CsA, necrotic cells decreased significantly, whereas apoptotic cells did not, which demonstrates the intermediary role of RIP3 in CsA-induced necroptotic process (Fig. 6).

2.4. Role of ROS in CsA-induced necroptosis of NRK-52E cells

Given that ROS production is required for CsA-induced cytotoxicity in HK-2 cells, LLC-PK1, and other renal proximal tubular cells, we hypothesized that ROS production through the RIP1 and RIP3 pathways is the most important mediator in CsA-induced necroptosis of NRK-52E cells. As shown in Fig. 7, Nec-1, as a specific PIR1 inhibitor, effectively inhibited CsA-induced ROS production. Moreover, RIP3 depletion in NRK-52E cells reduced the ROS concentration in the CsA-treated cells (Fig. 8). Of note, NAC, as a powerful radical scavenger, also reduced the ROS levels in the CsA-treated cells

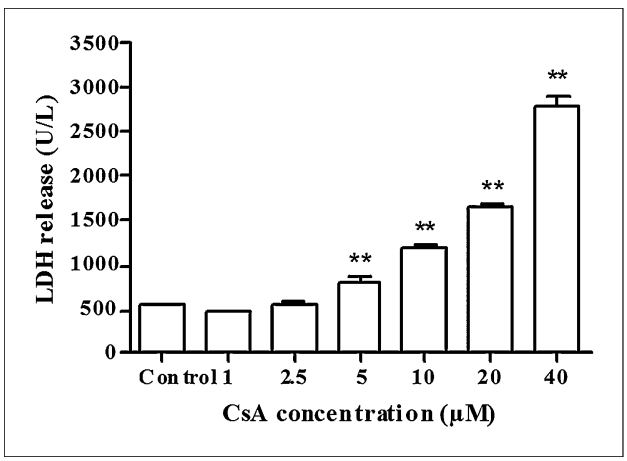

(A)

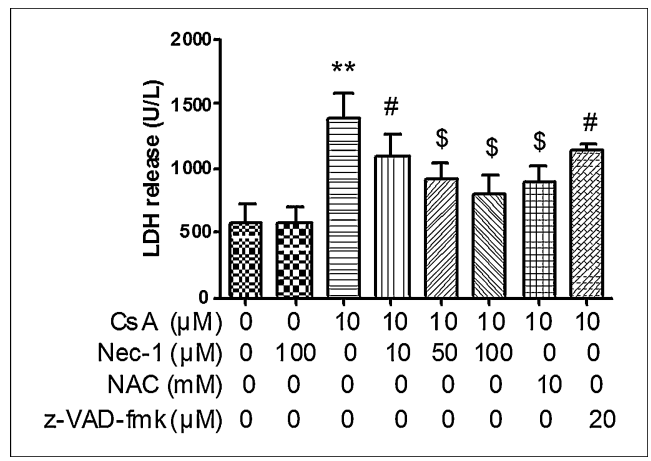

(B)

Fig. 2: Cytotoxicity of CsA in NRK-52E cells, as determined by LDH release. (A) NRK-52E cells were exposed to CsA (0, 1, 2.5, 5, 10, 20, and 40 μM) for 24 h. (B) NRK-52E cells were incubated with Nec-1 (10, 50, and 100 μM), z-VAD-fmk (20 μM) or NAC (10 mM) for 0.5 h prior to exposure to CsA (10 μM) for 24 h. Values are mean ± SD of measurements of nine separate NRK-52E cell cultures. Number of experiments (n = 3). vs. the control group; *$p < 0.01$ vs. the control group; $^{\#}$ $p < 0.05$ vs. the CsA group; $^{\$}$ $p < 0.05$ vs. the CsA group

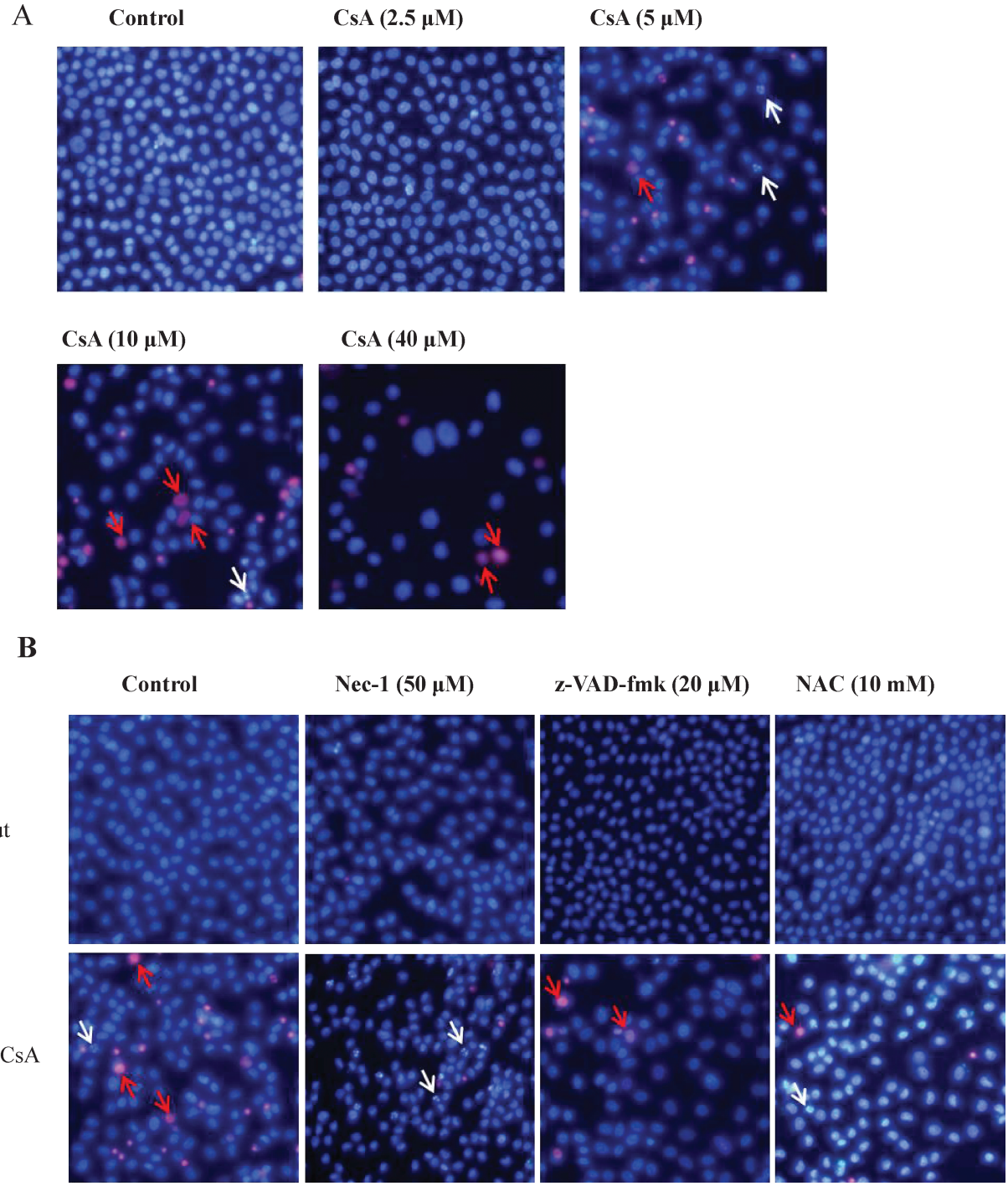

Fig. 3: Nec-1 or NAC protected against CsA-induced apoptosis and necrosis measured by Hoechst 33342 and PI Double Staining. (A) NRK-52E cells were exposed to CsA (0, 2.5, 5, 10, and 40 μM) for 24 h. (B) NRK-52E cells were incubated with Nec-1 (50 μM), z-VAD-fmk (20 μM) or NAC (10 mM) for 0.5 h prior to exposure to CsA (10 μM) for 24 h. Then, cells were stained with cell membrane-permeable (Hoechst 33342; blue) and -impermeable (propidium iodide; red). Images were obtained with a fluorescent microscope. White arrows indicate apoptotic cells and red arrows indicate necrotic cells. Original magnification: × 200

(Fig. 7) and effectively inhibited CsA-induced LDH release (Fig. 2B), and significantly attenuated the number of necrotic cells (Fig. 3B and Fig. 4). The results clearly indicate that CsA promotes ROS production in NRK-52E cells through the RIP1 and RIP3 pathways, leading to oxidative stress and cytotoxicity.

3. Discussion

A previous study showed that renal proximal tubular cells are the major target of CsA-induced nephrotoxicity in both humans and animal models. CsA treatment induces a loss of the brush border of renal proximal tubular cells and causes proximal tubule injury (Burdmann et al. 2003). In contrast, whether CsA-induced necrotic cell death can be regulated has not been studied yet. Recent evidence has indicated an alternative cell death process, necroptosis, a category type of programmed cell death (Degterev et al. 2005; Zhang et al. 2009; Cho et al. 2009). Necroptosis is characterized by a rapid loss of plasma membrane integrity, which could be specifically inhibited by Nec-1. The specificity of Nec-1 in inhibiting necroptosis has been well established on the following aspects (Degterev et al. 2005; Teng et al. 2005): (1) Nec-1 specially inhibits necroptosis, but does not inhibit apoptosis; (2) the specificity of Nec-1 in inhibiting necroptosis is also well defined by extensive structure–activity relationship analysis; (3) Nec-1 allosterically inhibits the kinase activity of

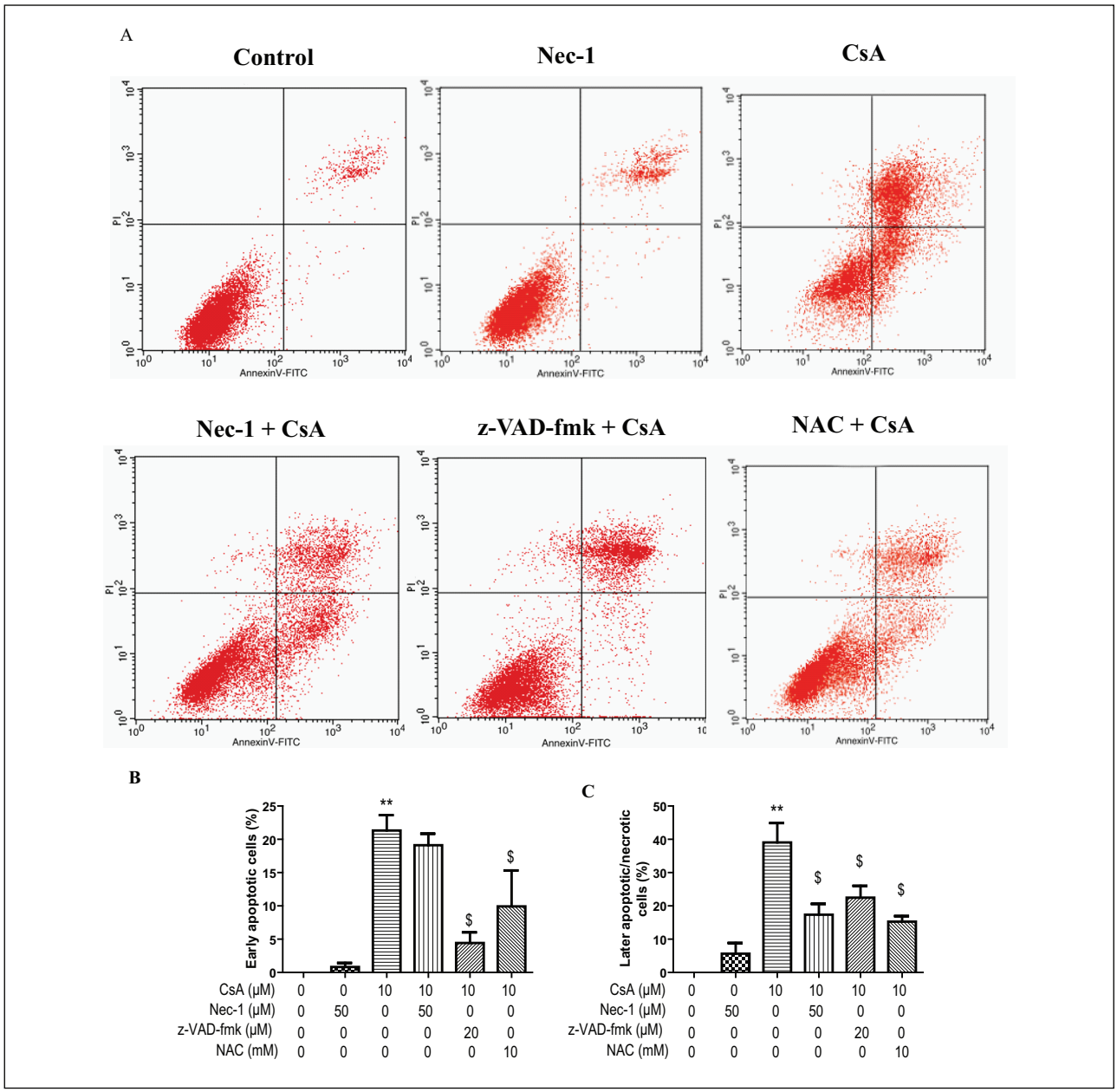

Fig. 4: Nec-1 and NAC protected NRK-52E cells against CsA-induced apoptosis and necrosis. NRK-52E cells were incubated with Nec-1 (50 μM), z-VAD-fmk (20 μM) or NAC (10 mM) for 0.5 h prior to exposure to CsA (10 μM) for 24 h. Then, the cells stained with stained with Annexin V-FITC solution (5 μl) and propidium iodide (PI, 5 μl) solution were measured by flow cytometry. (A) Representative results from triplicate experiments are shown. (B) Bar graph represents percentages of early apoptotic cells death. (C) Bar graph represents percentages of late apoptotic/necrotic cells death. Data are expressed as mean ± SD (n = 3). $^{**}p < 0.01$ vs. control group; $^{\$}p < 0.01$ vs. CsA alone

RIP1. Thus, Nec-1 can be used to determine whether cell death is necroptosis. In the current study, Nec-1 was used as a tool to examine whether necroptosis contributed CsA-induced renal proximal tubular cell death.

LDH is a cytoplasmic enzyme and is released to the extracellular medium whenever the cell membrane is damaged. The LDH level in the culture supernate is a marker for necrosis (Wroblewski and Ladue 1955). In the present study, LDH release into the culture medium was found to be significantly elevated after treatment with CsA, and this elevation was concentration dependent. However, Nec-1 pretreatment efficiently inhibited the LDH release triggered by CsA in the NRK-52E cell system. Even the lowest nec-1 concentration (10 μM) significantly reduced the LDH leakage, and at 100 μM, Nec-1 reversed the LDH release induced by CsA almost to the level of the control. These results demonstrate that Nec-1 has cytoprotective effects against CsA-induced toxicity. In the morphological study of the cytotoxic effects of CsA on NRK-52E cells, typical apoptotic bodies and necrotic cells with PI stained intact cell nuclei were detected

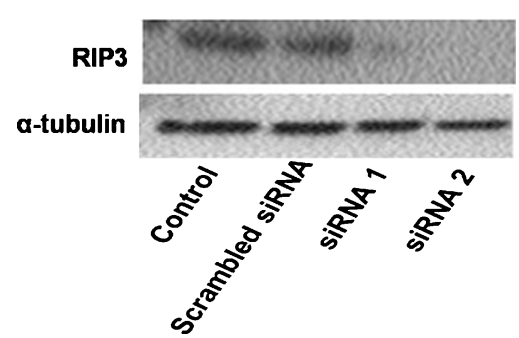

Fig. 5: Knockdown of RIP3 expression in NRK-52E cells by siRNA. Rat RIP3-specific siRNA (no. 1, no. 2), or unspecific "scrambled" siRNA was transfected into NRK-52E cells using Lipofectamine 2000. As the control, transfection was performed using only Lipofectamine without any siRNA. Cell lysates were prepared and analyzed for RIP3 expression through western blot analysis. Rat anti-α-tubulin antibodies were used as the internal control

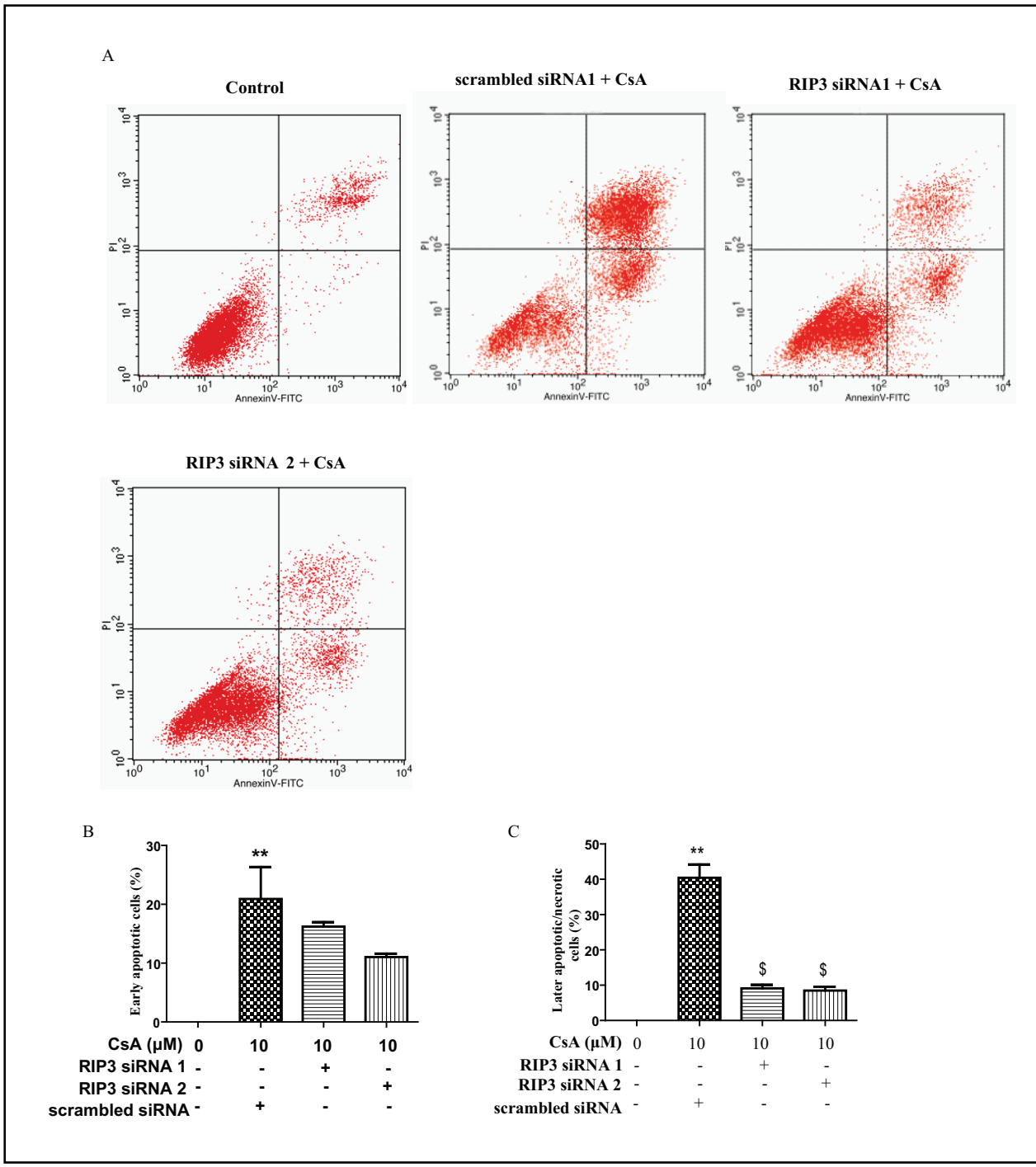

Fig. 6: Inhibition of cell death in NRK-52E cells by RIP3-siRNA transfection. Cells were transfected with nonspecific "scrambled" siRNA or RIP3-siRNA (no.1, no.2) for 48 h and then exposed to CsA (10 μM) for 24 h. Meanwhile, cells transfected with transfection reagent only were used as a control group. (A) Representative results from triplicate experiments are shown. (B) Bar graph represents percentages of early apoptotic cells death. (C) Bar graph represents percentages of late apoptotic/necrotic cells death. Data are expressed as mean ± SD (n = 3). $^{**}p < 0.01$ vs. the control group; $^{\$}p < 0.01$ vs. the CsA alone

in the CsA-treated group. As a pancaspase inhibitor, z-VAD-fmk decreased the CsA-induced apoptotic bodies, but not the necrotic cells with PI stained intact cell nuclei. On the contrary, the number of necrotic cells decreased significantly in the Nec-1 pretreated groups. To confirm further the protective effects of Nec-1, apoptosis and necrosis were analyzed by flow cytometry. Similarly, CsA induced cell apoptosis and necrosis simultaneously. Nec-1 specifically inhibited the necrosis caused by CsA but not in apoptosis. All these results suggest that necroptosis is involved in CsA-induced cell death in the renal proximal tubular cell. As discovered recently, necroptosis is an alternative form of programmed cell death. In some instances, the selective inhibition of necroptosis by Nec-1 may revert to apoptotic cell death (Han et al. 2009). In the current study, Nec-1 was also found to inhibit necroptosis but cannot facilitate apoptosis. The precise mechanism requires further study.

The pivotal role of RIP3 in the signal transduction cascade of necrosis has been reported (Zhang et al. 2009; He et al. 2009; Cho et al. 2009; Vandenabeele et al. 2010). Their studies revealed that RIP3 kinase functions with RIP1 at the step that determines apoptosis, necroptosis, or cell survival. Stimulation of the Fas/TNFR receptor family triggers the canonical 'extrinsic' apoptotic pathway, whereas in their absence, intracellular apoptotic signaling and high expression level of RIP3 render cells permissive to necroptosis. We characterized the involvement of RIP3 in CsA-induced necrosis using small interfering

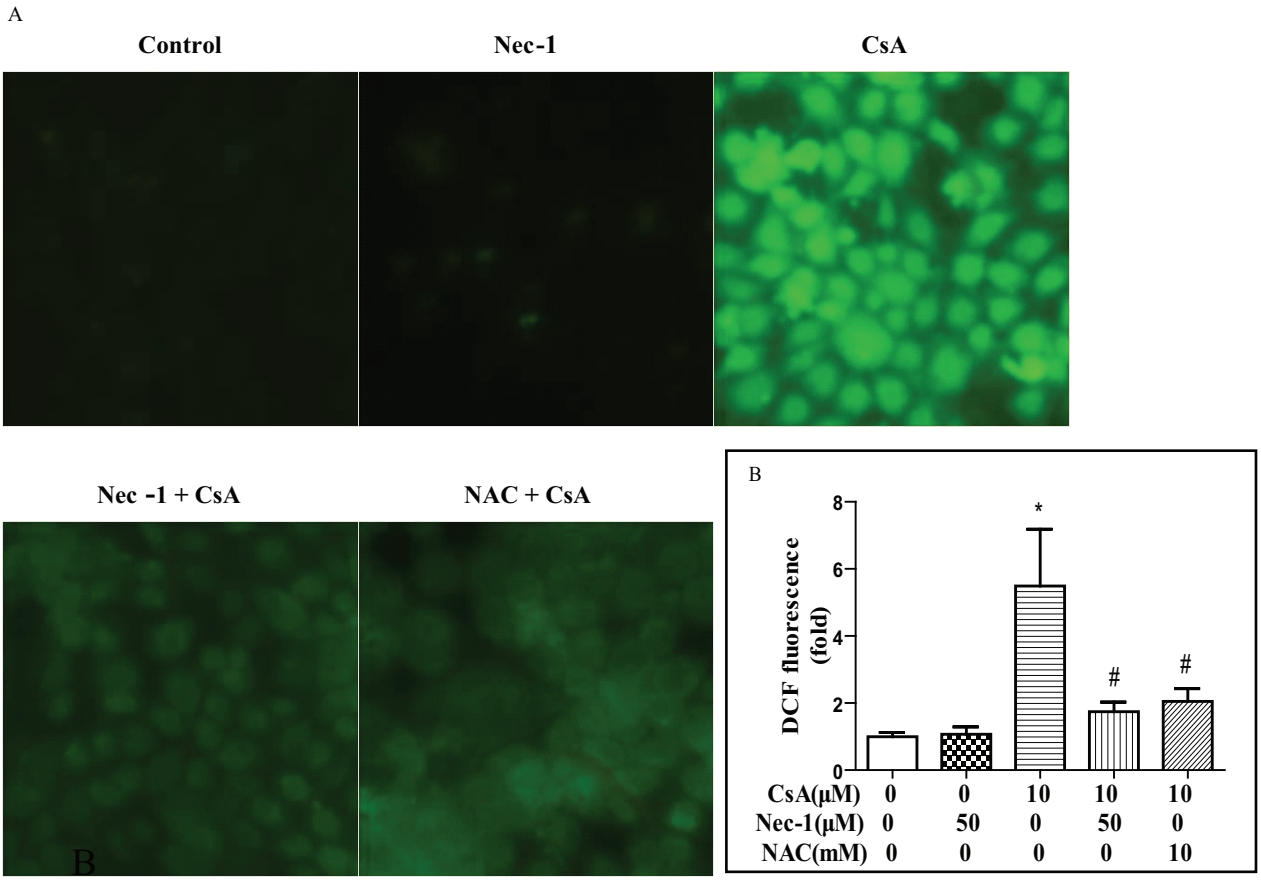

Fig. 7: Inhibitory effects of Nec-1 or NAC on intracellular ROS accumulation after exposure to CsA. NRK-52E cells were incubated with Nec-1 (50 μM) or NAC (10 mM) for 0.5 h prior to exposure to CsA (10 μM) for 24 h. Then, the cells stained with stained with 2′-7′-dichlorofluorescein (DCFH-DA) for 30 min. (A) Images were obtained with a fluorescent microscope (Magnification: × 200). (B) The graph shows the DCF fluorescence intensity as analyzed by multimode microplate reader as an indication of the ROS levels in the NRK-52E cells. Data are expressed as mean ± SD (n=3). *$p<0.01$ vs the control group; #$p<0.01$ vs the CsA alone

RNA. As expected, the CsA-induced necrosis was almost completely inhibited in the cells transfected with RIP3-siRNA. The results indicate that RIP3 participates in CsA-induced necroptosis. Necroptosis was initiated by death ligand binding to its receptor. Previous studies have shown that CsA increases Fas expression in cultured tubular cells (Justo et al. 2003; Healy et al. 1998), and increased FasL and Fas expression has been reported in chronic CsA nephrotoxicity (Lee et al. 2004; Shihab et al. 2005; Li et al. 2004; Healy et al. 1998; Yang et al. 2002). RIP1 and RIP3 are serine/threonine kinases. The kinase activity of RIP1 and RIP3 are required for stable RIP1 and RIP3 association to activate necroptosis. Unfortunately, the phosphorylation or dephosphorylation mechanisms of RIP3 and RIP1 remain unclear. CaN is a Ca^{2+}-calmodulin–dependent serine/threonine protein phosphatase. In the current study, RIP3 knockdown was found to have reduced CsA-induced necroptosis. However, RIP3 expression was not increased after the CsA treatment. Whether CsA induced Fas expression or stabilized the RIP1–RIP3 complex through inhibitor CaN, resulting in necroptosis, requires verification.

Many studies have suggested that disproportionate ROS production leads to necroptosis (Song et al. 2011; Thapa et al. 2011; Niu et al. 2009). The role of ROS in CsA-induced necrosis using the thiol antioxidant N-acetyl cysteine (NAC) was examined. A significant ROS overproduction was found in CsA-treated NRK-52E cells. Co-culture with NAC, a commonly used ROS scavenger, reduced the intracellular ROS levels and almost completely suppressed the CsA-induced cell death. Nec-1, although not a radical scavenger (Xu et al. 2007), effectively blocked the CsA-induced ROS generation. RIP3 siRNA also blocked the CsA-induced ROS generation, which suggests that ROS was produced through the RIP1 and RIP3 pathways in CsA-induced NRK-52E cells. Taken together, these data clearly indicate that ROS generation through the RIP1and RIP3 pathways is critical for CsA-induced necroptosis.

In the current study, Nec-1 and small interference RNA technique were used to reveal that CsA induces necroptosis in NRK-52E cells and that RIP3 is involved in CsA-induced necroptosis. In addition, ROS generation is critical for CsA-induced necroptosis. Most importantly, our study provides a new way of preventing and treating cyclosporin nephrotoxicity.

4. Experimental

4.1. Chemicals

High-glucose Dulbecco's modified Eagle's medium (DMEM), fetal bovine serum (FBS), penicillin, and streptomycin were obtained from Gibco. Nec-1 was purchased from Alexis. Hoechst 33342, propidium iodide (PI), dimethyl sulfoxide (DMSO), 3-(4,5-dimethyithiazol-2-yl)-2,5-diphenyl-tetrazolium bromide (MTT), 2′,7′-dichlorofluorescein diacetate (DCFH-DA), N-acetyl cysteine (NAC), and an LDH assay kit were purchased from the Beyotime Institute of Biotechnology (Haimen, China). Annexin V/propidium iodide (PI) apoptosis detection kit was obtained from Keygen Biotech. Co. Ltd (Nanjing, China). Anti-RIP3 antibodies were bought from Abcam Ltd. (Cambridge, UK). CsA, pancaspase inhibitor z-VAD-fmk, and anti-α-tubulin antibodies were purchased from Sigma Chemical Co. (St. Louis, MO, USA). Lipofectamine 2000 and Opti-MEM medium were purchased from Invitrogen.

4.2. Cell culture

NRK-52E cells were seeded into 6-well, 24-well, or 96-well plates at 37 °C in ATCC-modified DMEM containing 4.5 g/L glucose and 1.5 g/L sodium bicarbonate. It was supplemented with 10% fetal bovine serum, 100 U/mL penicillin, and 100 U/mL streptomycin in an atmosphere of 5% CO_2 and 95% air.

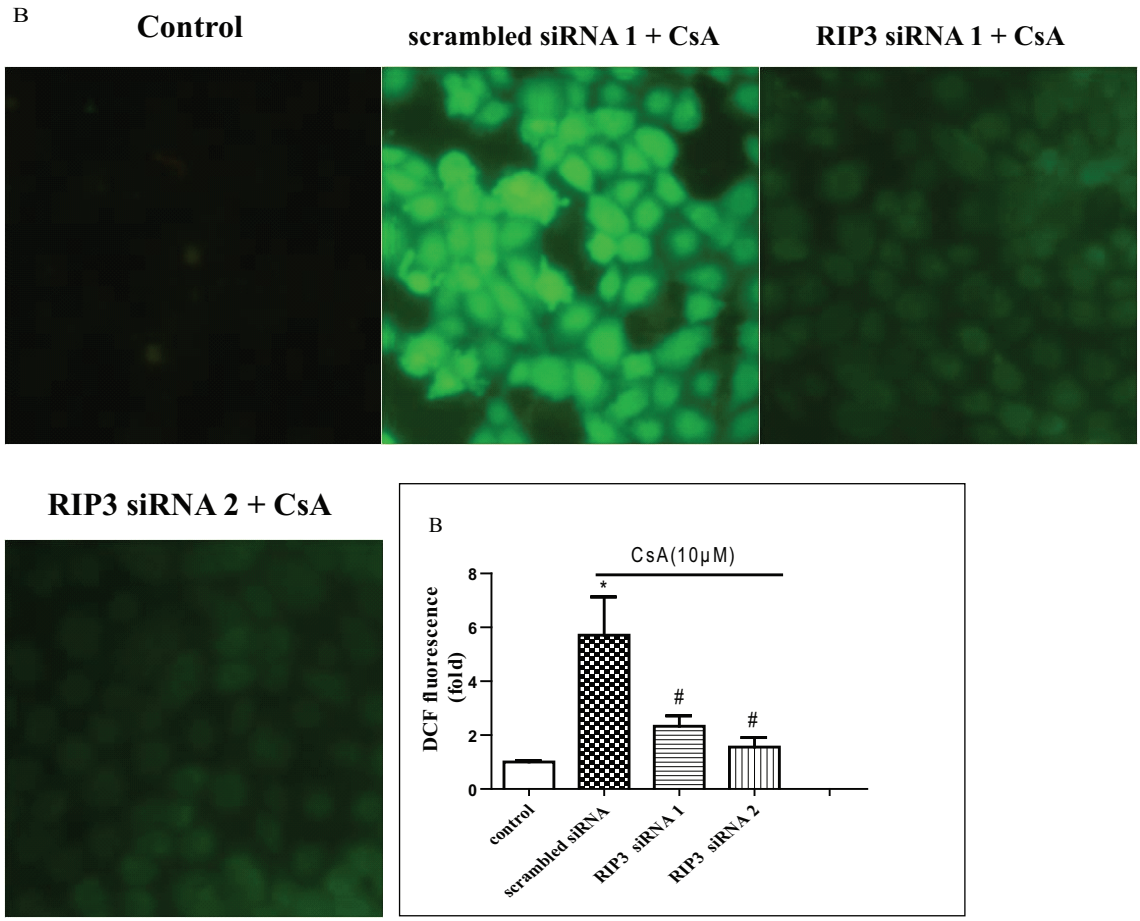

Fig. 8: Inhibitory effects of RIP3 siRNA on intracellular ROS accumulation after exposure to CsA as analyzed under fluorescence microscopy or a multimode microplate reader using DCFH-DA. Cells were transfected with nonspecific "scrambled" siRNA or RIP3-siRNA (no.1, no.2) for 48 h and then exposed to CsA (10 μM) for 24 h. Meanwhile, cells transfected with transfection reagent only were used as a control group. Then, the cells stained with stained with 2′-7′-dichlorofluorescein (DCFH-DA) for 30 min. (A) Images were obtained with a fluorescent microscope (Magnification: × 200). (B) The graph shows the DCF fluorescence intensity as analyzed by multimode microplate reader as an indication of the ROS levels in the NRK-52E cells. Data are expressed as mean ± SD (n=3). *$p<0.01$ vs the control group; #$p<0.01$ vs the CsA alone

4.3. Cell viability assay

Cell viability was measured by MTT reduction assays. Briefly, approximately 5×10^3 cells were plated onto each well of a 96-well plate for 24 h, followed by treatment with different CsA concentrations for a further 24 h. After incubation, 20 μL of MTT dye solution (5 mg/mL in PBS, pH 7.4) was added to wells containing 180 μL of growth medium. After 4 h of incubation at 37 °C, the medium was replaced with 200 μL of DMSO. After gently shaking at 37 °C for 10 min, MTT reduction was quantified spectrophotometrically at 570 nm using an Infinite M200 microplate reader. The assay results were expressed as the percentage of treated cells relative to the controls.

4.4. Lactate dehydrogenase (LDH) leakage assay

LDH is an enzyme widely present in the cytosol. When plasma membrane integrity is disrupted, LDH leaks into culture media and its extracellular level is elevated (Wroblewski and Ladue 1955). LDH assay was carried out by the LDH assay kit according to the manufacturer's protocol. In brief, NRK-52E cells were seeded into 24-well culture plates at a density of 0.5×10^5 cells/well in the medium and allowed to grow until approximately 80% confluent. The cells were then starved and synchronized for 12 h. Subsequently, the cells were exposed to 0, 1, 2.5, 5, 10, 20, and 40 μM CsA for 24 h. In another set of experiments, the cells were pretreated with Nec-1 (10, 50, and 100 μM), z-VAD-fmk (20 μM) or NAC (10 mM) for 0.5 h, and were then treated with CsA (10 μM) for 24 h. After the exposure was completed, the LDH levels in the media were measured by determining the LDH activity (measured spectrophotometrically by NADH oxidation at 440 nm).

4.5. Hoechst 33342/PI double staining

Cellular apoptosis or necrosis was assessed with Hoechst 33342/PI staining and subsequent analysis under fluorescence microscopy. Briefly, 3×10^5 cells/well were seeded into 6-well plates. The cells were treated with different concentrations of CsA (0, 2.5, 5, 10 and 40 μM) for 24 h or pretreated with Nec-1 (50 μM), z-VAD-fmk (20 μM), or NAC (10 mM) for 0.5 h, followed by CSA (10 μM) treatment for 24 h. The cells were subsequently treated with CsA (10 μM) for 24 h and then stained with Hoechst 33342 and PI for 15 min. The stained cells were observed under an IX71 inverted fluorescence microscope.

4.6. Flow cytometry analysis for apoptosis and necrosis

Apoptotic and necrotic cell deaths were analyzed by an Annexin V [fluorescein isothiocyanate (FITC)-conjugated]/PI apoptosis kit using FACScan flow cytometer (Becton Dickingson, San Jose, CA, USA). Briefly, the cells were harvested and resuspended in 500 μL binding buffer after treatment. Then, the cells were incubated with 5 μL Annexin V-FITC in the dark at 37 °C for 15 min, and 10 μL propidium iodide (PI, 50 mg/mL) was added into the cell suspension and incubated for an additional 5 min. The cells were immediately analyzed by FACS Calibur Flow Cytometry. For all the samples, the fluorescence of 10,000 cells was gated and counted. The percentages of the cells in the lower right (early apoptotic cells) and upper right (late apoptotic/necrotic cells) region of the scatter plot of Annexin V-FITC were calculated for comparison.

4.7. RIP3-siRNA transfection and treatment

The targeting sequences of two different siRNA and unspecific scrambled siRNA were purchased from the Ribo (Guangzhou, China). The siRNA sequences against the target gene were as follows: RIP3-siRNA no.1 sense, 5′-GGAAAGGCUUCUAAAGCAA-3′; antisense, 5′-UUGCUUUAGAAGCCUUUCC-3′; RIP3-siRNA no.2 sense, 5-′GCUGGA GUUCUG-AGCCUAA-3′; antisense, 5′-UUAGGCUCAGAACUCCAGC-3. Transfection of cells was performed by using Lipofectamine 2000 according to the manufacturer's specifications. Briefly, the cells were seeded into 6-well culture plates at a density of 2×10^5 cells/well in the medium and allowed to grow until approximately 70% confluence, the culture medium was carefully replaced with 1500 μL

of fresh Opti-MEM medium, and then 500 μL of the transfection mixture was added to the medium. The cells were transfected with a final concentration of 100 nM of siRNA. After 6 h, the medium was changed to DMEM with serum and the transfected cells were cultured for 48 h. Transfected cells were then treated with CsA (10 μM) for 24 h for flow cytometry analysis. Knockdown of the target molecule, RIP3, was monitored by western blot analysis.

4.8. Western blotting analysis

After treatment, the cells were washed twice with cold PBS and lysed in RIPA extraction buffer (1 × PBS, 0.5% deoxycholic acid sodium salt, 1% Triton X-100, 0.1% SDS, 1 mM PMSF) for 25 min on ice. The lysates were centrifuged for 10 min at 4 °C to remove debris, and the protein concentrations were determined via a Bradford protein assay. Equivalent amounts of total protein were separated using 12% sodium dodecyl sulfate polyacrylamide gel electrophoresis and electroblotted onto polyvinylidene difluoride membranes (Millipore Co., Billerica, MA, USA). The membranes were blocked in 5% non-fat milk in TBST (10 mM Tris–HCl [pH 8.0], 150 mM NaCl, and 0.1% Tween-20) for 2 h, then incubated with the primary antibodies: rabbit anti-RIP3 antibodies (1:1000 dilution), or mouse anti-α-tubulin antibodies (1:10000 dilution) at 4 °C overnight. Subsequently, the immunoblots were incubated with secondary antibodies conjugated with horseradish peroxidase at room temperature for 1 h. Antibody binding was detected using an Enhanced Chemiluminescence Detection Kit (ECL).

4.9. Fluorescent measurement of intracellular ROS

ROS generation was measured using the oxidation-sensitive fluorescent probe DCFH-DA as previously described (de Souza et al. 2007). The cells (5×10^3/per well on a 96-well tissue culture plate) were cultured for 24 h in 100 μL of complete medium, and then cells were pretreated with Nec-1 (50 μM) or NAC (5 mM) for 0.5 h and then exposed to CsA (10 μM) for 4 h. In another set of experiments, the cells were transfected with RIP3-siRNA or scrambled si-RNA for 48 h and were then treated with CsA (10 μM) for 4 h. After the CsA-treatment, 100 μL of DCFH-DA (10 μM) in serum-free medium was added. At 20 min after incubation, the probe-containing medium was removed and washed with PBS. The ROS levels were determined by fluorescence microscopy or by Multimode Microplate Reader (BMG LABTECH, Germany) at an excitation wavelength of 488 nm, and fluorescence emission was measured at 525 nm.

4.10. Data analysis

All data are expressed in mean values ± standard deviation (SD); differences between experimental groups were analyzed by paired Student t-tests. A P-value < 0.05 was considered significant.

Acknowledgements: The work was supported by the Key Projects in the National Science and Technology Pillar Program of China (Grant No. 2008BAI55B03). The authors also appreciate the finacial support provided by Science and Technology Foundation of Guangdong province (Grant No. 2007B030704008).

References

Bakker RC, van Kooten C, van de Lagemaat-Paape ME, Daha MR, Paul LC (2002) Renal tubular epithelial cell death and cyclosporin A. Nephrol Dial Transplant 17: 1181–1188.

Borel JF, Baumann G, Chapman I, Donatsch P, Fahr A, Mueller EA, Vigouret JM (1996) *In vivo* pharmacological effects of ciclosporin and some analogues. Adv Pharmacol 35: 115–246.

Burdmann EA, Andoh TF, Yu L, Bennett WM (2003) Cyclosporine nephrotoxicity. Semin Nephrol 23: 465–476.

Cho YS, Challa S, Moquin D, Genga R, Ray TD, Guildford M, Chan FK (2009) Phosphorylation-driven assembly of the RIP1-RIP3 complex regulates programmed necrosis and virus-induced inflammation. Cell 137: 1112–1123.

Degterev A, Huang Z, Boyce M, Li Y, Jagtap P, Mizushima N, Cuny GD, Mitchison TJ, Moskowitz MA, Yuan J (2005) Chemical inhibitor of nonapoptotic cell death with therapeutic potential for ischemic brain injury. Nat Chem Biol 1: 112–119.

Han W, Xie J, Li L, Liu Z, Hu X (2009) Necrostatin-1 reverts shikonin-induced necroptosis to apoptosis. Apoptosis 14: 674–686.

He S, Wang L, Miao L, Wang T, Du F, Zhao L, Wang X (2009) Receptor interacting protein kinase-3 determines cellular necrotic response to TNF-alpha. Cell 137: 1100–1111.

Healy E, Dempsey M, Lally C, Ryan MP (1998) Apoptosis and necrosis: mechanisms of cell death induced by cyclosporine A in a renal proximal tubular cell line. Kidney Int 54: 1955–1966.

Justo P, Lorz C, Sanz A, Egido J, Ortiz A (2003) Intracellular mechanisms of cyclosporin A-induced tubular cell apoptosis. J Am Soc Nephrol 14: 3072–3080.

Kahan BD (1992) Immunosuppressive therapy. Curr Opin Immunol 4: 553–560.

Lee SY, Jo SK, Cho WY, Kim HK, Won NH (2004) The effect of alpha-melanocyte-stimulating hormone on renal tubular cell apoptosis and tubulointerstitial fibrosis in cyclosporine A nephrotoxicity. Transplantation 78: 1756–1764.

Li C, Lim SW, Sun BK Choi BS, GLowacka S, Cox A, Kelly D, Kim YS, Kim J, Bang BK, Yang CW (2004) Expression of apoptosis-related factors in chronic cyclosporine nephrotoxicity after cyclosporine withdrawal. Acta Pharmacol Sin 25: 401–411.

Majno G, Joris I (1995) Apoptosis, oncosis, and necrosis. An overview of cell death. Am J Pathol 146: 3–15.

Mihatsch MJ, Ryffel B, Hermle M, Brunner FP, Thiel G. (1986) Morphology of cyclosporine nephrotoxicity in the rat. Clin Nephrol 25 Suppl 1: S2–8.

Myers BD, Sibley R, Newton L, Tomlanovich SJ, Boshkos C, Stinson E, Luetscher JA, Whitney DJ, Krasny D, Coplon NS et al. (1988) The long-term course of cyclosporine-associated chronic nephropathy. Kidney Int 33: 590–600.

Nakamura T, Nozu K, Iijima K, Yoshikawa N, Moriya Y, Yamamori M, Kako A, Matsuo M, Sakurai A, Okamura N, Ishikawa T, Okumura K, Sakaeda T (2007) Association of cumulative cyclosporine dose with its irreversible nephrotoxicity in Japanese patients with pediatric-onset autoimmune diseases. Biol Pharm Bull 30: 2371–2375.

Nickeleit V, Zeiler M, Gudat F, Thiel G, Mihatsch MJ (1998) Histological characteristics of interstitial renal allograft rejection. Kidney Blood Press Res 21: 230–232.

Niu Q, Zhang QL, Zheng JP, Liu CY, Wang L (2009) [Role of necroptosis in aluminum induced SH-SY5Y cell death]. Zhonghua Yu Fang Yi Xue Za Zhi 43: 132–136.

Racusen LC (1993) Tubular injury in human kidneys: pathologic findings and pathogenic mechanisms. Clin Investig 71: 858–860.

Shihab FS, Bennett WM, Yi H, Andoh TF (2005) Effect of pirfenidone on apoptosis-regulatory genes in chronic cyclosporine nephrotoxicity. Transplantation 79: 419–426.

Song KJ, Jang YS, Lee YA, Kim KA, Lee SK, Shin MH (2011) ROS-dependent necroptosis in Jurkat T cells induced by pathogenic free-living Naegleria fowleri. Parasite Immunol 33: 390–400.

Teng X, Degterev A, Jagtap P, Xing X, Choi S, Denu R, Yuan J, Cuny GD (2005) Structure-activity relationship study of novel necroptosis inhibitors. Bioorg Med Chem Lett 15: 5039–5044.

Thapa RJ, Basagoudanavar S, Nogusa S, Irrinki K, Mallilankaraman K, Slifker MJ, Beg AA, Madesh M, Balachandran S (2011) NF-{kappa}B protects cells from interferon-{gamma}-induced RIP1-dependent necroptosis. Mol Cell Biol 31: 2934–2946.

Vandenabeele P, Galluzzi L, Vanden Berghe T, Kroemer G (2010) Molecular mechanisms of necroptosis: an ordered cellular explosion. Nat Rev Mol Cell Biol 11: 700–714.

Wroblewski F, Ladue JS (1955) Lactic dehydrogenase activity in blood. Proc Soc Exp Biol Med 90: 210–213.

Xu X, Chua CC, Kong J, Kostrzewa RM, Kumaraguru U, Hamdy RC, Chua BH (2007) Necrostatin-1 protects against glutamate-induced glutathione depletion and caspase-independent cell death in HT-22 cells. J Neurochem 103: 2004–2014.

Yang CW, Faulkner GR, Wahba IM, Christianson TA, Bagby GC, Jin DC, Abboud HE, Andoh TF, Bennett WM (2002) Expression of apoptosis-related genes in chronic cyclosporine nephrotoxicity in mice. Am J Transplant 2: 391–399.

Yu PW, Huang BC, Shen M, Quast J, Chan E, Xu X, Nolan GP, Payan DG, Luo Y (1999) Identification of RIP3, a RIP-like kinase that activates apoptosis and NFkappaB. Curr Biol 9: 539–542.

Zhang DW, Shao J, Lin J, Zhang N, Lu BJ, Lin SC, Dong MQ, Han J (2009) RIP3, an energy metabolism regulator that switches TNF-induced cell death from apoptosis to necrosis. Science 325: 332–336.